Equation of state of hexagonal-close-packed rhenium in the terapascal regime

G. L. Rech, J. E. Zorzi, and C. A. Perottoni*
Universidade de Caxias do Sul, 95070-560 Caxias do Sul, RS, Brazil

(Received 1 July 2019; revised manuscript received 15 October 2019; published 19 November 2019)

All-electron density functional theory calculations were performed aiming to determine the equation of state and the dependence with pressure of the c/a ratio and the anisotropic compressibility for hexagonal-close-packed rhenium. Calculations were carried out up to maximum compression of 0.46, and the resulting total energy versus volume is well described by a Vinet equation of state with $B_0 = 367(5)$ GPa and $B_0' = 4.64(3)$, valid up to 1.5 TPa. The agreement with two recent experimental studies [S. Anzellini *et al.*, Equation of state of rhenium and application for ultra high pressure calibration, J. Appl. Phys. **115**, 043511 (2014); T. Sakai *et al.*, High pressure generation using double-stage diamond anvil technique: Problems and equations of state of rhenium, High Pressure Res. **38**, 107 (2018)] supports their conclusion that the pressure in previous experiments with a double-stage diamond-anvil cell [L. Dubrovinsky *et al.*, Implementation of micro-ball nanodiamond anvils for high-pressure studies above 6 Mbar, Nat. Commun. **3**, 1163 (2012)] was significantly overestimated.

DOI: 10.1103/PhysRevB.100.174107

I. INTRODUCTION

Rhenium is a dense, refractory, and rare (the 77th most abundant element on Earth's crust, and the last stable element to be discovered) transition metal, which belongs to group 7 of the periodic table of the elements [1–3]. At ambient conditions, rhenium crystallizes in a hexagonal-close-packed (hcp) structure, space group $P6_3/mmc$, with two atoms per unit cell [4–6]. Despite rhenium being relatively soft and ductile, rhenium strength increases more than any other pure metal under plastic deformation [7–10]. The exceptional work hardening and the high melting point of rhenium make it particularly suited for use as a high strength gasket in high-pressure experiments with the diamond-anvil cell (DAC) [9,11]. Besides providing a container for the sample, the metallic gasket also supports laterally the diamond anvils and, particularly in the case of rhenium gaskets, it further provides a way to estimate pressure, by x-ray diffraction from the material at the edge of the gasket hole [9,12–16]. Indeed, x-ray diffraction of the gasket material, along with the Raman spectrum of the diamond anvil at the point of contact with the sample, are becoming increasingly useful methods for pressure calibration, along with widely used internal standards, such as gold [16–18]. In fact, approaching the terapascal regime statically has only become possible at the cost of considerably reducing sample size, thus making use of internal standards less desirable [16]. Also, other methods for pressure estimation in the DAC, including the ruby technique and the Raman shift of cubic boron nitride, are unfeasible at such ultrahigh pressures or are yet to become more widely used [9,13,19]. Recent improvements in anvil design, with claims of the upper limit of static pressures attained with the DAC now approaching 1 TPa, only make more urgent the increasing need for reliable methods to estimate the pressure in this extended regime [20–26].

The ability to estimate the pressure in diamond-anvil cell experiments by x-ray-diffraction analysis of the gasket inner rim is very dependent on the accuracy of currently available equations of state (EOSs). However, in the case of rhenium, previous theoretical and experimental studies were restricted to pressures well below 1 TPa. Prior computational studies on rhenium's EOS include linear muffin-tin orbital (LMTO) relativistic calculations (without spin-orbit contribution) [27], full-potential (FP) LMTO density functional theory (DFT) calculations in the local-density approximation (LDA) [28], FP linearized augmented plane-wave (LAPW) calculations in both LDA and generalized gradient approximation (GGA) [29], norm-conserving pseudopotential (NC-PP) LDA/GGA DFT [30], and projector augmented wave (PAW) DFT/LDA calculations [31]. All these computational studies were restricted to the compression range $V/V_0 \geqslant 0.7$. Moreover, the stability of hcp Re with respect to a possible transition to a body-centered structure has been previously assessed up to 1 TPa [32]. The behavior of Re under high static pressures has also been the subject of several experimental studies, starting with a pioneering work by Bridgman [8] and extending up to very recent times [12,16,20,22,33–36].

Despite these several computational and experimental studies, controversies have arisen on a proposed equation of state for rhenium that is valid in the regime of ultrahigh pressures [16,20,22]. Indeed, pressures around 0.64 TPa have been claimed to be achieved with a double-stage modified diamond-anvil cell by Dubrovinsky *et al.* [20]. In the study carried out by Dubrovinsky *et al.*, the pressure was estimated on the basis of the gold EOS and a fourth-order Birch-Murnaghan EOS was proposed for rhenium [20]. A pressure of 640(17) GPa was estimated for the maximum compression reached in that study, $V/V_0 = 0.633$. However, later

*caperott@ucs.br

experimental studies on the Re EOS have suggested that the maximum pressure achieved in the high-pressure x-ray-diffraction experiments with rhenium in the double-stage DAC may have been overestimated by 150 to 200 GPa [16,22].

In this paper, all-electron DFT calculations were performed aiming to determine an athermal EOS of Re that is valid in the terapascal regime. Despite the higher computational cost, an all-electron method was chosen to avoid potential pitfalls due to core overlap and failure of the pseudopotential approximation in the high compression regime here explored [37–39]. Besides giving support to recent experimental results regarding rhenium's compression under very high pressure, the DFT calculations here reported unveil the effect of pressure on the lattice-parameter c/a ratio and the anisotropic compressibility of hcp Re.

II. COMPUTATIONAL METHODOLOGY

A. DFT calculations

DFT calculations were performed using a linearized augmented plane-wave plus several local orbitals basis set, as implemented in the full-potential all-electron EXCITING code [40]. Calculations were performed in the athermal limit, i.e., at 0 K and without the inclusion of zero-point energy. The calculations were performed with the PBEsol exchange-correlation functional [41]. Core electrons were treated as fully relativistic, while valence electrons were treated as spin polarized, according to the scalar-relativistic Schrödinger equation, within infinite-order regular approximation [42]. Calculations included relativistic spin-orbit effects [40]. The muffin-tin (MT) part of the wave-function basis set is expanded in terms of products of spherical harmonics and radial functions, in a radial mesh of 1000 points. In the interstitial region, the wave function is expanded in a base of plane-wave functions, up to a maximum angular momentum $l_{\max} = 12$ [40]. The muffin-tin radius was set as $R_{\mathrm{MT}} = 1.8$ bohrs. Within the MT region, wave functions, density, and potential were also expanded up to $l_{\max} = 12$. The plane-wave basis set size for the wave-function expansion outside the MT sphere is defined as $R_{\mathrm{MT}}|\mathbf{G}+\mathbf{k}|_{\max} = 12$, for a $\mathbf{k}$ grid of $31 \times 31 \times 19$, and a maximum length of the reciprocal-lattice vector $|\mathbf{G}|$ equal to 30 bohr^{-1}. The occupancies of the Kohn-Sham states are calculated using a Gaussian approximation to the Dirac delta function, with a 0.5-μhartree width. The criterion for total energy convergence is set to 0.25 μhartree. These are very tight computational conditions, similar to those used in recent studies aiming to gauge the precision and reproducibility in DFT calculations of solids [43,44]. The input and some relevant output files were deposited in the NoMaD repository [45,46].

B. Equation of state

The equilibrium c/a ratio for different values of the unit-cell volume was obtained as the point of minimum of a second-degree polynomial fitted to total energy versus c/a ratio. Rhenium's equilibrium volume at zero pressure V_0, bulk modulus B_0, and pressure derivative B_0' were estimated using the isothermal Vinet EOS [47,48],

$$P(V) = \frac{3B_0 x}{(1-x)^2} e^{\eta x}, \tag{1}$$

where $x = 1 - (V/V_0)^{1/3}$ and $\eta = \frac{3}{2}(B_0' - 1)$. The Vinet EOS has been chosen because it has been shown to suitably describe the behavior of materials over large compression ranges [49]. Integrated with respect to volume, the Vinet EOS yields an expression for the energy variation upon an isothermal volume change,

$$\Delta E(V) = -\int_{V_0}^{V} P(V)dV,$$

$$E(V) = E(V_0) + \frac{9B_0V_0}{\eta^2}[1 + e^{\eta x}(\eta x - 1)]. \tag{2}$$

C. Linear compressibilities

For the calculation of linear compressibilities, fourth-degree polynomials were fitted to lattice parameters a and c versus unit-cell volume data. From these, the linear compressibility parallel to the a axis was obtained as $\beta_a = -(\frac{\partial \ln a}{\partial V})(\frac{\partial V}{\partial P})$ and, correspondingly, for β_c. The derivative $\partial V/\partial P$ was calculated assuming the Vinet EOS. For comparison, the ratio of the adiabatic linear compressibilities β_c/β_a was estimated from experimental elastic constants using expressions (18)–(21) from Lv *et al.* [30].

III. RESULTS AND DISCUSSION

The crystal structure of Re, for a given unit-cell volume, is defined uniquely by the ratio of the unit-cell parameters c/a. The equilibrium c/a ratio for hcp Re was determined for 12 different unit-cell volumes, ranging from 90 to 225 bohrs^3. The resulting total energy versus c/a ratio curves are exhibited in Fig. 1. The point of minimum of each panel in Fig. 1, i.e., the optimized c/a ratio for each unit-cell volume, was then used to represent the total energy versus unit-cell volume in Fig. 2. Fitting of the integrated Vinet EOS [2] to total energy versus unit-cell volume yields the bulk modulus and its pressure derivative, $\mathrm{B}_0 = 367(5)$ GPa= and $\mathrm{B}_0' = 4.64(3)$, respectively. The equilibrium unit-cell volume, in the athermal limit, is estimated as $V_0 = 196.7(3)$ bohrs^3. A comparison is made with previous computational and experimental results in Table I. Our results for rhenium's unit-cell volume and bulk modulus, while well within the range of previous theoretical results, are slightly under- and overestimated, respectively, in comparison with experimental results. This opposite trend is commonly observed in DFT calculations, irrespective of the chosen exchange-correlation functional [50]. While previous computational studies of rhenium's EOS were restricted to a maximum compression of $V/V_0 = 0.7$, our calculations were extended up to $V/V_0 = 0.46$, corresponding to a pressure around 1.5 TPa.

Figure 3 shows that, except for very high-pressure data above 0.3 TPa, there is an excellent agreement between the Vinet EOS and previous experimental results for Re. A further comparison is made in Fig. 4 between the athermal EOS of rhenium, as obtained in this paper, and some recently experimental EOSs. In all cases, the volume versus pressure curves

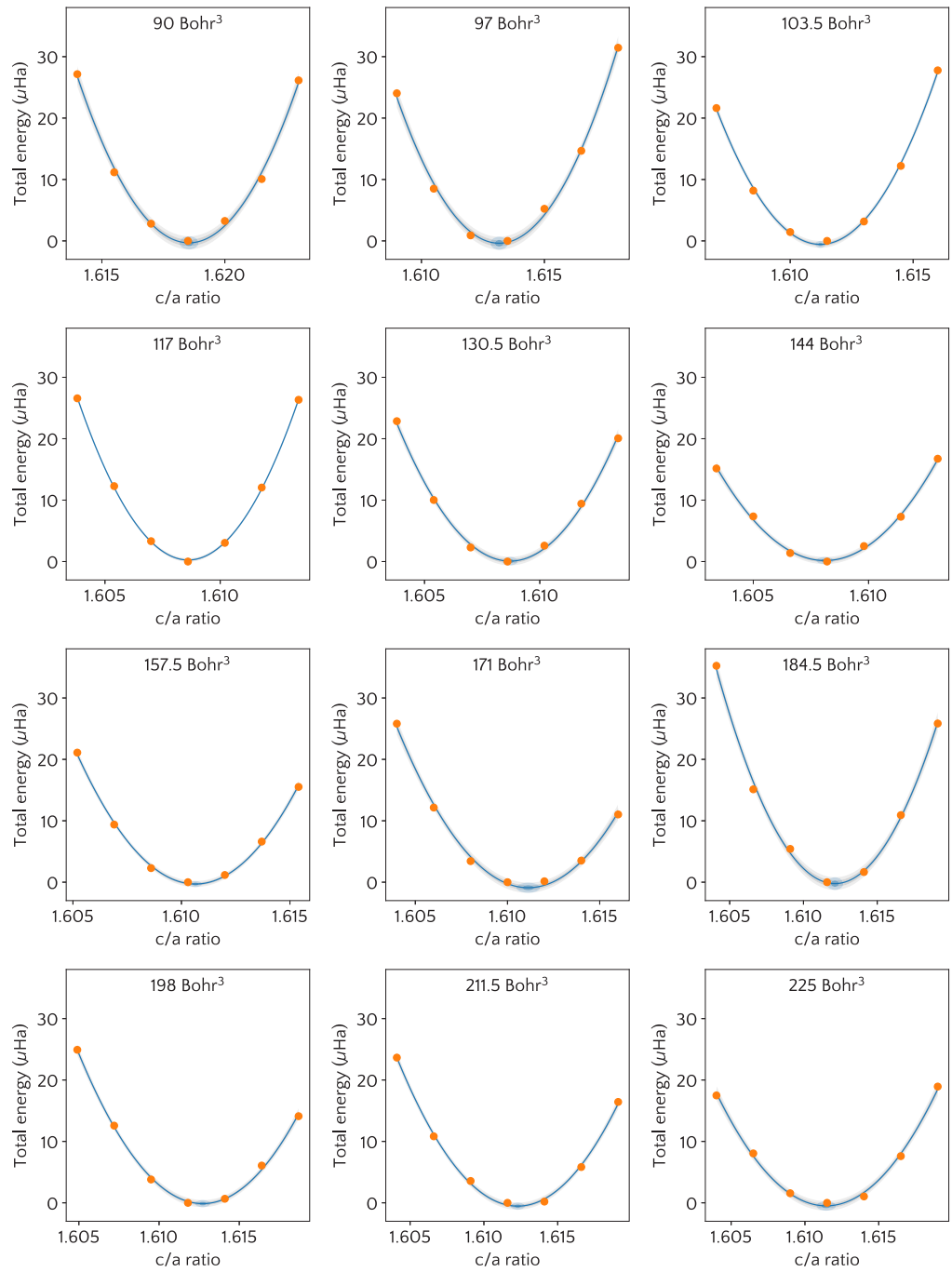

FIG. 1. Total energy with respect to the point of minimum vs c/a ratio for different unit-cell volumes of hcp Re. The solid lines represent a second-degree polynomial fitted to data. Dark and light gray bands represent the fitting 1σ and 2σ error bands, respectively. The dark and light blue spots represent the 1σ and 2σ interval around the point of minimum, respectively.

were extended up to $V/V_0 = 0.45$. The calculated relation between V/V_0 and pressure is similar to that of Anzellini *et al.* [16], and virtually identical to that of Sakai *et al.* [22]. This last observation holds despite the differences between the bulk modulus and its first pressure derivative, as obtained by us [$B_0 = 367(5)$ GPa and $B_0' = 4.64(3)$, respectively], and those of Sakai *et al.* [$B_0 = 358(10)$ GPa and $B_0' = 4.8(2)$, respectively]. The similarity of V/V_0 versus pressure curves, for different B_0 and B_0', is a symptom that these two parameters (usually along with V_0) are strongly correlated [56]. On the other hand, the EOS proposed by Dubrovinsky *et al.* [20] differs significantly from the others, leading to an overestimation of pressure for $V/V_0 < 0.8$ (i.e., for pressures above about 140 GPa). Indeed, for a compression $V/V_0 = 0.45$, the EOS proposed by Dubrovinsky *et al.* yields $P = 3.1$ TPa, almost twice the pressure estimated according to the other EOSs compared in Fig. 4 (1.57, 1.62, and 1.47 TPa for the EOSs proposed in this paper, by Sakai *et al.* [22], and by Anzellini *et al.* [16], respectively). It is noteworthy that the EOS of Dubrovinsky *et al.* [20] starts deviating towards overestimated

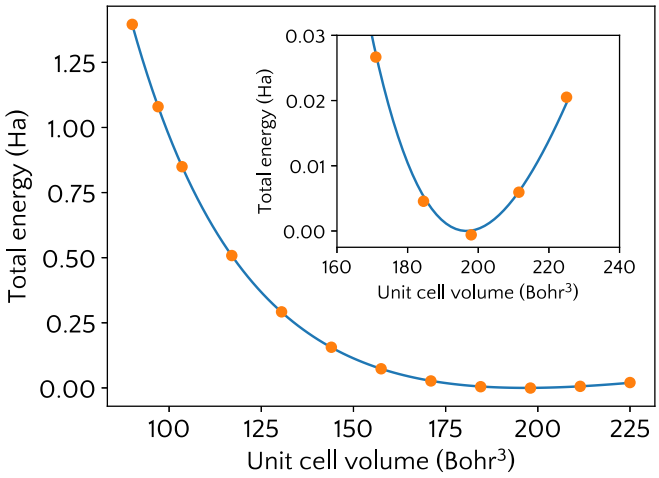

FIG. 2. Total energy with respect to the minimum energy vs unit-cell volume for rhenium, in the athermal limit. The line represents the fitted Vinet EOS. The inset shows an expanded view around the point of minimum energy.

pressures at just about the pressure above which results were obtained using a double-stage DAC [20]. In fact, the EOS here proposed is compatible with the Dubrovinski *et al.* data from a conventional DAC experiment [20], as can be seen in the inset of Fig. 3.

More often than not, the lattice-parameter ratio c/a for hcp Re has been considered to be virtually independent of pressure in both theoretical and experimental studies on the high-pressure behavior of rhenium (see, for instance, Refs. [12,29,30,33,35]). Exceptions to this are experimental studies conducted by Dubrovinsky *et al.* [20] and Anzellini *et al.* [16], who observed a reduction of c/a from about 1.615 to 1.612 (i.e., a 0.19% reduction) upon increasing pressure to 150 GPa [16,20]. Hints of a complex dependence of rhenium's c/a ratio on compression have also been found in previous FP-LMTO calculations [32]. The dependence of the c/a ratio with the unit-cell volume for hcp Re is shown in Fig. 5. In this figure it is also shown how the c/a ratio varies with pressure, as calculated using the Vinet EOS. The slope $d\ln(c/a)/dP$ averaged over the pressure range up to 150 GPa, $-9.7\,\mu\text{GPa}^{-1}$, should be compared to the value estimated from the high-pressure x-ray-diffraction results by Dubrovinsky *et al.* [20] (using a conventional DAC) and Anzellini *et al.* [16], namely, $-12\,\mu\text{GPa}^{-1}$ [16,20]. The small variation of the c/a ratio with pressure makes it hardly noticeable and both

TABLE I. Rhenium's theoretical and experimental zero pressure unit-cell volume (V_0), c/a ratio, and bulk modulus (B_0) and its first pressure derivative (B_0').

Reference	V_0 (bohrs^3)	c/a	B_0 (GPa)	B_0'
This work[a]	196.7(3)	1.6125(3)[b]	367(5)	4.64(3)
LMTO LDA [27]	198.4		372	5.41
FP-LMTO LDA [28]	197.5	1.628	447.3	
FP-LAPW LDA [29]	196.4	1.615	382	3.9
FP-LAPW GGA/PBE [29]	206.0	1.615	344	3.9
NC-PP LDA/Vosko [30]	196.96	1.61	389	4.52
NC-PP GGA/PBE [30]	198.16	1.608	376	4.58
PAW LDA/CA [31]	194.2	1.613	412	
Exp. (4.2 K) [51]	197.56			
Exp.[c,g] (4 K) [52]			371.5	
Exp.[d] (4.2 K) [53]			367.8(13)	
Exp. (RT[e]) [8]			371	
Exp.[d,f] (RT) [34]			368	
Exp.[g] (RT) [35]			360.3(15)	5.43(35)
Exp. (RT) [36]			360.3(15)[h]	5.43(35)
Exp. (RT) [54]	199.40(19)	1.6212(15)		
Exp. (RT) [7]	198.47(15)	1.6152(7)		
Exp. (RT) [16]	198.85(22)		352.6(80)	4.56(17)
Exp. (RT) [33]	198.6	1.614	350(15)	2.9(13)
Exp. (RT) [22]	198.9		358(10)	4.8(2)
Exp. (RT) [12]		1.613	372	4.05
Exp. (RT) [55]	198.3			4.6
Exp. (RT) [20]	198.81(7)	1.615	342(6)[i]	6.15(15)

[a]The figures in parentheses are the estimated uncertainties (1σ) in the last digit, as obtained by fitting the integrated Vinet EOS (2).
[b]Calculated from the polynomial fitted to data as in Fig. 5.
[c]As given by Zha, Bassett, and Shim [51].
[d]Adiabatic bulk modulus calculated from the elastic constants as $B_s = \frac{2}{9}(C_{11} + C_{12} + 2C_{13} + C_{33}/2)$ [28].
[e]Room temperature.
[f]As given by Fast, Wills, Johansson, and Eriksson [28].
[g]Isothermal bulk modulus estimated from the adiabatic bulk modulus.
[h]Fourth-order Birch-Murnaghan EOS with $B_0'' = -0.0616(42)$.
[i]Fourth-order Birch-Murnaghan EOS with $B_0'' = -0.029(4)$.

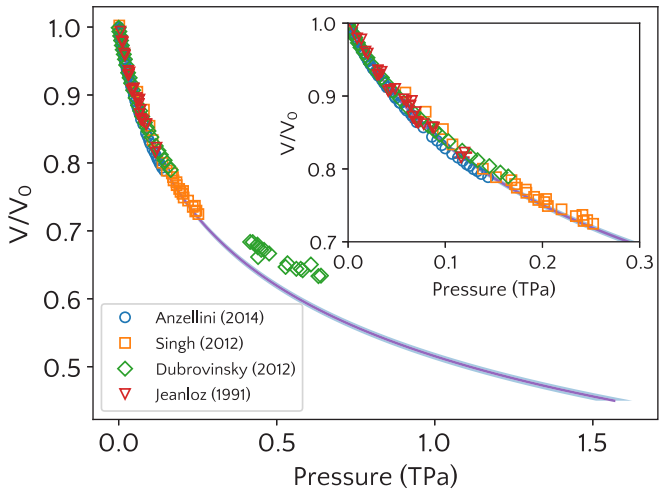

FIG. 3. Comparison of the athermal EOS for rhenium with experimental data from Anzellini *et al.* [16], Singh *et al.* [10], Dubrovinsky *et al.* [20], and Jeanloz *et al.* [36]. The blue shaded solid line represents the Vinet EOS with a 2σ confidence interval band. The inset shows an expanded view of the experimental data and the Vinet EOS below 0.3 TPa. Experimental error bars (when available in the original references) are always smaller than the symbols used to represent data.

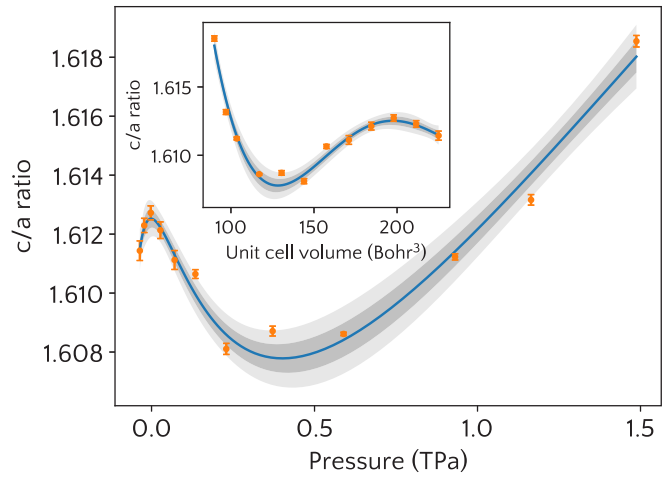

FIG. 5. Calculated dependence of the ratio of the unit-cell lattice parameters c/a of rhenium on pressure and volume (in the inset). The solid line in the inset represents a fourth-degree polynomial fitted to data. The continuous line in the main plot was obtained from the polynomial expression for c/a as a function of volume, which was converted into a pressure scale with the Vinet EOS. Dark and light gray bands represent the fitting 1σ and 2σ confidence interval, respectively.

computationally and experimentally challenging to account for. Indeed, even over the large 1.5-TPa pressure range here explored, the c/a ratio spanned a very small interval from 1.608 to about 1.618, i.e., a total variation of just 0.6%. The larger c/a variation of -1.3% (from 1.615 to 1.595) in going from ambient to 640 GPa in a double-stage DAC, as reported by Dubrovinsky *et al.* [20], was not confirmed by our DFT calculations. Rhenium's c/a ratio exhibits a maximum near ambient pressure, decreasing with pressure up to a shallow minimum ($c/a = 1.608$, 0.3% smaller than the zero pressure equilibrium ratio) around 0.41 TPa ($V/V_0 \approx 0.65$, to be compared to a minimum at $V/V_0 \approx 0.75$, as reported by Verma *et al.* [32]), above which the c/a ratio keeps

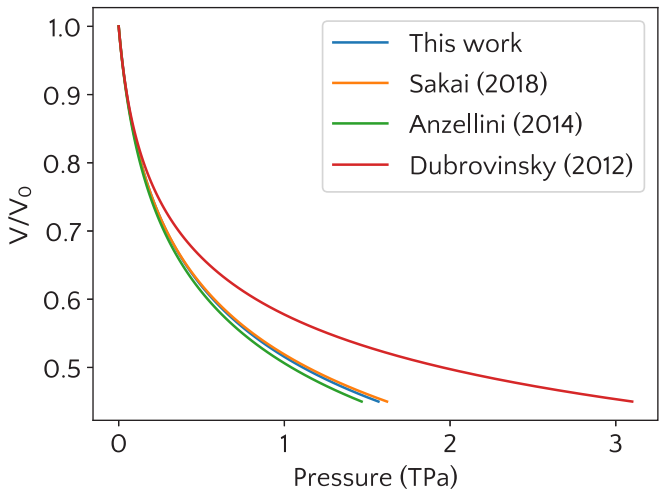

FIG. 4. Comparison between the athermal EOS for rhenium, as proposed in this paper, and those of Sakai *et al.* [22], Anzellini *et al.* [16], and Dubrovinsky *et al.* [20].

increasing until the maximum compression here explored, $V/V_0 = 0.46$. This interesting behavior could only be made apparent due to a very strict set of computational conditions, which allowed unambiguous determination of the point of minimum in total energy versus c/a ratio curves, at constant volume (Fig. 1), even for total-energy variations of only a few tens of μhartree. The c/a ratio for Re remains below the value for an *ideal* hexagonal-close-packed structure, $c/a = \sqrt{8/3} \approx 1.633$, over all the compression range here explored.

A point of minimum c/a ratio as a function of pressure has been reported for other hcp metals, including osmium [57,58], beryllium [59], cobalt [60], samarium, and dysprosium [61]. In fact, the pressure dependence of rhenium's c/a ratio is similar to that exhibited by osmium, for which a minimum is observed around 75 GPa, for an overall variation less than 1% up to about 200 GPa [58]. Noteworthy, in their study of osmium under high pressure, Perreault *et al.* [58] did not find compelling evidence of a point of minimum in the c/a ratio at approximately 150 GPa, as previously reported by Dubrovinsky *et al.* [57]. On the other hand, the results reported by Dubrovinsky *et al.* did not show any evidence of the broad minimum in the c/a ratio for osmium near 75 GPa. These observations exemplify how difficult it is to obtain robust evidence on the effect of pressure on the c/a ratio for hcp metals. Anomalies in the pressure dependence of the c/a ratio for hcp metals, including an inversion of the first pressure derivative, have been attributed, albeit not always conclusively (as demonstrated by the difficulty in asserting even the very existence of the anomalies), to electronic topological transitions, core-level crossing transition, and changes in the magnetic behavior [57,60]. In the case of rhenium, the nearly constant c/a ratio makes it easier to determine the (approximate) unit-cell volume by x-ray diffraction and, thus, the estimation of pressure in experiments with the

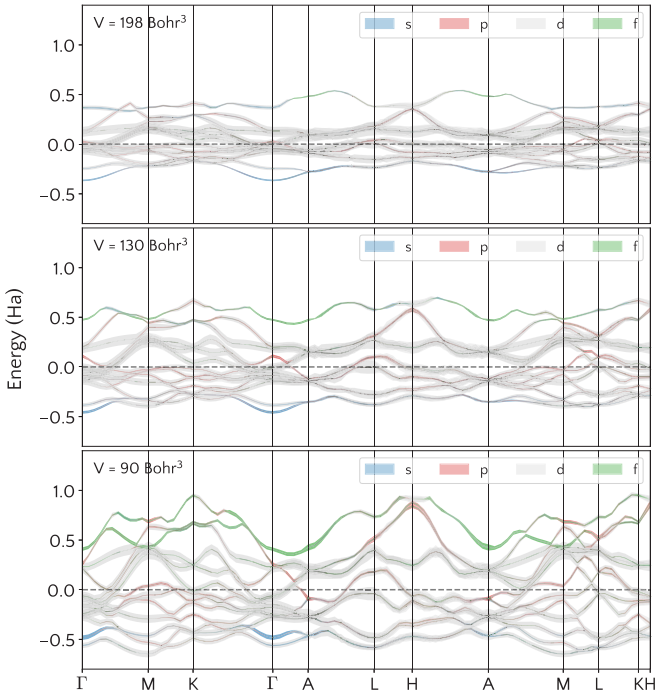

FIG. 6. Electronic band structure of rhenium near the Fermi level for three selected volumes, from top to bottom: 198, 130, and 90 bohrs^3. Line thickness is proportional to the s, p, d, or f character of each band. Energy is expressed relative to Fermi level.

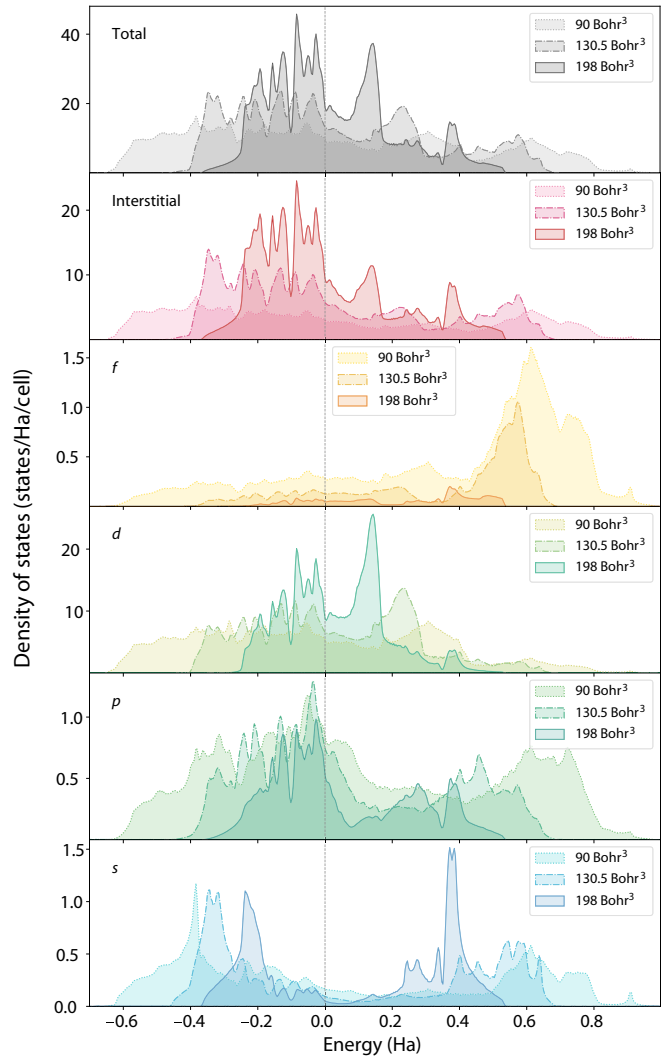

FIG. 7. From top to bottom: Total, interstitial, and partial electronic density of states (DOS) per one spin direction of Re for three unit-cell volumes: 198, 130, and 90 bohrs^3. Energy is expressed relative to Fermi level.

diamond-anvil cell and rhenium's gaskets. In fact, by knowing the lattice parameter a (for instance, from the lattice spacing of one or more Bragg peaks in the x-ray diffraction pattern of the gasket material) the unit-cell volume of rhenium at 1.5 TPa, calculated for a constant c/a ratio as given at zero pressure, differs by only -0.34% of the actual value, for a volume reduction of 54%. In this hypothetical example, the approximate unit-cell volume translates into an estimated pressure that is about 1% greater than the value obtained by taking into account the c/a variation with pressure.

The band structure and density of states (DOS) of Re for three different unit-cell volumes are represented in Figs. 6 and 7, respectively (see also Supplemental Material Figs. S1 and S2 [62]). The chosen volumes (198, 130, and 90 bohrs^3) correspond, in this order, to 2.4 GPa, 372 GPa (near ambient pressure and the point of minimum c/a, respectively), and the maximum compression explored in this paper, 1.49 TPa.

The calculated band structure of Re resembles that of Mattheiss, including the band splitting along the L-H-A direction due to spin-orbit coupling [63]. There is a pressure-induced enhancement of the p and f hybridization with the top $5d$ bands of Re, as can be seen both in Fig. 6 and in the f density of states in Fig. 7. Also noticeable is the crossing of the bottom of the $6s$ conduction band, which is the lowest Γ state in the top two panels of Fig. 6, with a portion of a branch of a $5d$ band. The Fermi energy for rhenium increases logarithmically with pressure, from around 0.76 hartree at ambient pressure up to 1.8 hartree near 1.49 TPa.

The total DOS spreads out upon increasing pressure, spanning roughly 0.9 hartree around the Fermi energy (E_F) near ambient pressure and 1.5 hartree at 1.49 TPa. The total DOS spreading is accompanied by a decrease in the number of states at the Fermi level, nearly halving from ambient pressure to 1.49 TPa. Indeed, the total DOS at the Fermi level increases linearly with the unit-cell volume over the entire pressure range here explored.

Rhenium's total density of states for $V = 198$ bohrs^3 exhibits a deep valley some 0.1 hartree below E_F [63], a common feature of hcp metal DOS [[64], p. 490]. The dip in the DOS becomes less evident upon pressure increase, to the point of not being present at all at the upper pressure limit. The DOS not only spreads out but also becomes featureless at increasingly higher pressures.

At zero pressure, in the athermal limit, the linear compressibilities of rhenium parallel to the unit-cell a axis ($\beta_a = 0.910\,\mathrm{TPa}^{-1}$) and c axis ($\beta_c = 0.911\,\mathrm{TPa}^{-1}$), despite being very similar, are not identical [35]. The ratio $\beta_c/\beta_a = 1.001$ can be compared to the adiabatic ratios 1.012(7) and 0.987(8), as estimated from the elastic constants of Fischer and Dever [52] and Shepard and Smith [53], respectively (both as given

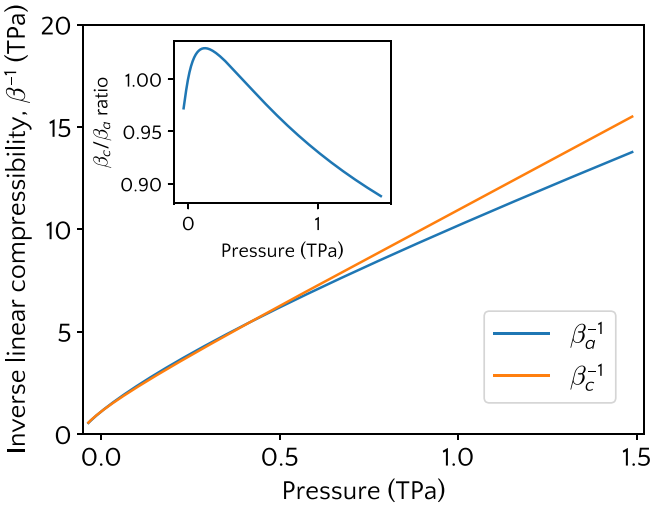

FIG. 8. Dependence with pressure of rhenium's inverse linear compressibilities parallel to the unit-cell a axis (β_a^{-1}) and c axis (β_c^{-1}). The inset shows the ratio β_c/β_a as a function of pressure.

by Manghnani *et al.* [35]); the adiabatic room temperature given by Manghnani, Katahara, and Fischer, 1.009(8) [35]; and the isothermal room-temperature ratio estimated from data by Liu, Takahashi, and Bassett, 1.03(11) [33]. This ratio reaches a maximum ($\beta_c/\beta_a \approx 1.03$) near 0.13 TPa, above which β_c continuously decreases relative to β_a (see Fig. 8).

IV. CONCLUSIONS

An equation of state for rhenium was proposed based on all-electron DFT calculations carried out up to $V/V_0 = 0.46$ (about 1.5 TPa). The influence of pressure upon rhenium's c/a ratio and anisotropic compressibility was also unambiguously determined. According to the proposed EOS, the maximum pressure in previous x-ray diffraction experiments with rhenium, using a double-stage DAC [20], is overestimated by ≈200 GPa, in quantitative agreement with latter experimental studies by Anzellini *et al.* [16] and Sakai *et al.* [22]. The agreement between the proposed Vinet EOS and experimental data obtained under reasonably isostatic conditions suggests the use of the former over the large pressure range now attainable with specially designed diamond-anvil cells. The athermal Vinet EOS, obtained over an extended pressure range up to 1.5 TPa, can arguably be used near room temperature. A further extension, aiming to obtain an isothermal EOS applicable at much higher temperatures, can be pursued either computationally [65–69] or by using experimental thermophysical parameters [51] to account for the effects of temperature.

ACKNOWLEDGMENTS

We gratefully acknowledge support from the Brazilian agencies Conselho Nacional de Desenvolvimento Científico e Tecnológico, Grants No. 304831/2014-0 and No. 305253/2018-2 (C.A.P.), and Grants No. 304675/2015-6 and No. 305528/2018-1 (J.E.Z.); Programa de Apoio a Núcleos de Excelência Fundação de Amparo à Pesquisa do Estado do Rio Grande do Sul; and Coordenação de Aperfeiçoamento de Pessoal de Nível Superior, Brasil, Finance Code 001. This research was made possible also thanks to computational resources provided by the Centro de Computação Científica (NCC/GridUNESP), Universidade Estadual de São Paulo (UNESP), Núcleo Avançado de Computação de Alto Desempenho da COPPE, Universidade Federal do Rio de Janeiro, and Centro Nacional de Supercomputação of the Universidade Federal do Rio Grande do Sul. Thanks are due also to Ney Lemke (Departamento de Física e Biofísica, Instituto de Biociências de Botucatu, IBB/UNESP), who granted us access to the NCC/GridUNESP computational resources.

[1] W. Noddack, Die ekamangane, Naturwissenschaften **13**, 567 (1925).
[2] J. Emsley, *Nature's Building Blocks: An A-Z Guide to the Elements* (Oxford University, New York, 2003).
[3] I. L. Shabalin, Rhenium, in *Ultra-High Temperature Materials I: Carbon (Graphene/Graphite) and Refractory Metals* (Springer, New York, 2014), pp. 317–357.
[4] V. M. Goldschmidt, Die krystallstruktur des rheniums, Naturwissenschaften **17**, 134 (1929).
[5] V. M. Goldschmidt, Kristallstruktur, gitterkonstanten und dichte des rheniums, Z. Phys Chem **2B**, 244 (1929).
[6] H. E. Swanson and E. Tatge, Standard x-ray diffraction powder patterns, Natl. Bur. Stand. **539**, 1 (1953).
[7] C. T. Sims, C. M. Craighead, and R. I. Jaffee, Physical and mechanical properties of rhenium, JOM **7**, 168 (1955).
[8] P. W. Bridgman, Miscellaneous effects of pressure on miscellaneous substances, in *Proceedings of the American Academy of Arts and Sciences* (American Academy of Arts & Sciences, 1955), Vol. 84, pp. 111–129.
[9] M. I. Eremets, *High Pressure Experimental Methods* (Oxford University, New York, 1996).
[10] A. K. Singh, J. Hu, J. Shu, H. K. Mao, and R. J. Hemley, Strength of rhenium from x-ray diffraction experiments under nonhydrostatic compression to 250 GPa, J. Phys. Conf. Ser. **377**, 012008 (2012).
[11] D. Schiferl, Temperature compensated high-temperature/high-pressure Merrill Bassett diamond anvil cell, Rev. Sci. Instrum. **58**, 1316 (1987).
[12] Y. K. Vohra, S. J. Duclos, and A. L. Ruoff, High-pressure x-ray diffraction studies on rhenium up to 216 GPa (2.16 Mbar), Phys. Rev. B **36**, 9790 (1987).
[13] G. Shen and H. K. Mao, High-pressure studies with x-rays using diamond anvil cells, Rep. Prog. Phys. **80**, 016101 (2017).
[14] P. Loubeyre, F. Occelli, and R. LeToullec, Optical studies of solid hydrogen to 320 GPa and evidence for black hydrogen, Nature (London) **416**, 613 (2002).
[15] C. Narayana, H. Luo, J. Orloff, and A. L. Ruoff, Solid hydrogen at 342 GPa: No evidence for an alkali metal, Nature (London) **393**, 46 (1998).
[16] S. Anzellini, A. Dewaele, F. Occelli, P. Loubeyre, and M. Mezouar, Equation of state of rhenium and application for ultra high pressure calibration, J. Appl. Phys. **115**, 043511 (2014).

[17] C. S. Zha, H. Liu, J. S. Tse, and R. J. Hemley, Melting and high P-T transitions of hydrogen up to 300 GPa, Phys. Rev. Lett. **119**, 075302 (2017).

[18] Y. Fei, A. Ricolleau, M. Frank, K. Mibe, G. Shen, and V. Prakapenka, Toward an internally consistent pressure scale, Proc. Natl. Acad. Sci. USA **104**, 9182 (2007).

[19] K. P. Esler, R. E. Cohen, B. Militzer, J. Kim, R. J. Needs, and M. D. Towler, Fundamental high-pressure calibration from all-electron quantum Monte Carlo calculations, Phys. Rev. Lett. **104**, 185702 (2010).

[20] L. Dubrovinsky, N. Dubrovinskaia, V. B. Prakapenka, and A. M. Abakumov, Implementation of micro-ball nanodiamond anvils for high-pressure studies above 6 Mbar, Nat. Commun. **3**, 1163 (2012).

[21] T. Sakai, T. Yagi, H. Ohfuji, T. Irifune, Y. Ohishi, N. Hirao, Y. Suzuki, Y. Kuroda, T. Asakawa, and T. Kanemura, High-pressure generation using double stage micro-paired diamond anvils shaped by focused ion beam, Rev. Sci. Instrum. **86**, 033905 (2015).

[22] T. Sakai, T. Yagi, T. Irifune, H. Kadobayashi, N. Hirao, T. Kunimoto, H. Ohfuji, S. Kawaguchi-Imada, Y. Ohishi, S. Tateno, and K. Hirose, High pressure generation using double-stage diamond anvil technique: Problems and equations of state of rhenium, High Press. Res. **38**, 107 (2018).

[23] B. Li, C. Ji, W. Yang, J. Wang, K. Yang, R. Xu, W. Liu, Z. Cai, J. Chen, and H.-k. Mao, Diamond anvil cell behavior up to 4 Mbar, Proc. Natl. Acad. Sci. USA **115**, 1713 (2018).

[24] A. Dewaele, P. Loubeyre, F. Occelli, O. Marie, and M. Mezouar, Toroidal diamond anvil cell for detailed measurements under extreme static pressures, Nat. Commun. **9**, 2913 (2018).

[25] E. F. O'Bannon, III, Z. Jenei, H. Cynn, M. J. Lipp, and J. R. Jeffries, Contributed review: Culet diameter and the achievable pressure of a diamond anvil cell: Implications for the upper pressure limit of a diamond anvil cell, Rev. Sci. Instrum. **89**, 111501 (2018).

[26] N. Dubrovinskaia, L. Dubrovinsky, N. A. Solopova, A. Abakumov, S. Turner, M. Hanfland, E. Bykova, M. Bykov, C. Prescher, V. B. Prakapenka, S. Petitgirard, I. Chuvashova, B. Gasharova, Y. L. Mathis, P. Ershov, I. Snigireva, and A. Snigirev, Terapascal static pressure generation with ultrahigh yield strength nanodiamond, Sci. Adv. **2**, e1600341 (2016).

[27] S. K. Sikka and V. Vijayakumar, Theoretical isothermal equation of state of rhenium, Phys. Rev. B **38**, 10926 (1988).

[28] L. Fast, J. M. Wills, B. Johansson, and O. Eriksson, Elastic constants of hexagonal transition metals: Theory, Phys. Rev. B **51**, 17431 (1995).

[29] G. Steinle-Neumann, L. Stixrude, and R. E. Cohen, First-principles elastic constants for the hcp transition metals Fe, Co, and Re at high pressure, Phys. Rev. B **60**, 791 (1999).

[30] M. B. Lv, Y. Cheng, Y. Y. Qi, G. F. Ji, and C. G. Piao, Elastic properties and phonon dispersions of rhenium in hexagonal-close-packed structure under pressure from first principles, Physica B **407**, 778 (2012).

[31] M. de Jong, D. L. Olmsted, A. van de Walle, and M. Asta, First-principles study of the structural and elastic properties of rhenium-based transition-metal alloys, Phys. Rev. B **86**, 224101 (2012).

[32] A. K. Verma, P. Ravindran, R. S. Rao, B. K. Godwal, and R. Jeanloz, On the stability of rhenium up to 1 TPa pressure against transition to the bcc structure, Bull. Mater. Sci. **26**, 183 (2003).

[33] L.-G. Liu, T. Takahashi, and W. A. Bassett, Effect of pressure and temperature on the lattice parameters of rhenium, J. Phys. Chem. Solids **31**, 1345 (1970).

[34] G. Simmons and H. Wang, *Single Crystal Elastic Constants and Calculated Aggregate Properties: A Handbook* (MIT, Cambridge, MA, 1971).

[35] M. H. Manghnani, K. Katahara, and E. S. Fischer, Ultrasonic equation of state of rhenium, Phys. Rev. B **9**, 1421 (1974).

[36] R. Jeanloz, B. K. Godwal, and C. Meade, Static strength and equation of state of rhenium at ultra-high pressures, Nature (London) **349**, 687 (1991).

[37] B. Winkler and V. Milman, Density functional theory based calculations for high pressure research, Z. Kristallogr. **229**, 112 (2014).

[38] C. J. Pickard and R. J. Needs, Ab initio random structure searching, J. Phys-Condens. Mat. **23**, 053201 (2011).

[39] P. R. Levashov, G. V. Sin'ko, N. A. Smirnov, D. V. Minakov, O. P. Shemyakin, and K. V. Khishchenko, Pseudopotential and full-electron DFT calculations of thermodynamic properties of electrons in metals and semiempirical equations of state, J. Phys. Condens. Mat. **22**, 505501 (2010).

[40] A. Gulans, S. Kontur, C. Meisenbichler, D. Nabok, P. Pavone, S. Rigamonti, S. Sagmeister, U. Werner, and C. Draxl, Exciting: A full-potential all-electron package implementing density-functional theory and many-body perturbation theory, J. Phys.: Condens. Matter **26**, 363202 (2014).

[41] J. P. Perdew, A. Ruzsinszky, G. I. Csonka, O. A. Vydrov, G. E. Scuseria, L. A. Constantin, X. Zhou, and K. Burke, Restoring the Density-Gradient Expansion for Exchange in Solids and Surfaces, Phys. Rev. Lett. **100**, 136406 (2008).

[42] K. G. Dyall and E. van Lenthe, Relativistic regular approximations revisited: An infinite-order relativistic approximation, J. Chem. Phys. **111**, 1366 (1999).

[43] K. Lejaeghere, G. Bihlmayer, T. Björkman, P. Blaha, S. Blügel, V. Blum, D. Caliste, I. E. Castelli, S. J. Clark, A. Dal Corso, S. de Gironcoli, T. Deutsch, J. K. Dewhurst, I. Di Marco, C. Draxl, M. Dułak, O. Eriksson, J. A. Flores-Livas, K. F. Garrity, L. Genovese *et al.*, Reproducibility in density functional theory calculations of solids, Science **351**, aad3000 (2016).

[44] A. Gulans, A. Kozhevnikov, and C. Draxl, Microhartree precision in density functional theory calculations, Phys. Rev. B **97**, 161105(R) (2018).

[45] NoMaD repository, https://www.nomad-coe.eu/ (2019) [accessed 28 May 2019].

[46] EXCITING input and output files, http://dx.doi.org/10.17172/NOMAD/2019.10.21-1 (2019).

[47] P. Vinet, J. Ferrante, J. H. Rose, and J. R. Smith, Compressibility of solids, J. Geophys. Res. Sol. EA **92**, 9319 (1987).

[48] R. J. Angel, M. Alvaro, and J. Gonzalez-Platas, EosFit7c and a Fortran module (library) for equation of state calculations, Z. Krist. Cryst. Mater. **229**, 405 (2014).

[49] R. E. Cohen, O. Gülseren, and R. J. Hemley, Accuracy of equation-of-state formulations, Am. Mineral. **85**, 338 (2000).

[50] F. Tran, J. Stelzl, and P. Blaha, Rungs 1 to 4 of DFT Jacob's ladder: Extensive test on the lattice constant, bulk modulus, and cohesive energy of solids, J. Chem. Phys. **144**, 204120 (2016).

[51] C. S. Zha, W. A. Bassett, and S. H. Shim, Rhenium, an in situ pressure calibrant for internally heated diamond anvil cells, Rev. Sci. Instrum. **75**, 2409 (2004).

[52] E. S. Fischer and D. Dever, Temperature dependence of elastic moduli of Ru, Re, Co, Dy, and En. A study of the elastic anisotropy-phase transformation relationship, T. Metall. Soc. AIME **239**, 48 (1967).

[53] M. L. Shepard and J. F. Smith, Elastic constants of rhenium single crystals in the temperature range 4.2°–298°K, J. Appl. Phys. **36**, 1447 (1965).

[54] R. Wasilevski, Physical and mechanical properties of rhenium, T. Metall. Soc. Aime **221**, 1081 (1961).

[55] T. S. Duffy, G. Shen, D. L. Heinz, J. Shu, Y. Ma, H. K. Mao, R. J. Hemley, and A. K. Singh, Lattice strains in gold and rhenium under nonhydrostatic compression to 37 GPa, Phys. Rev. B **60**, 15063 (1999).

[56] W. B. Holzapfel, Equations of state for high pressure phases, Rev. High Pres. Sci. Tech. **11**, 55 (2001).

[57] L. Dubrovinsky, N. Dubrovinskaia, E. Bykova, M. Bykov, V. Prakapenka, C. Prescher, K. Glazyrin, H.-P. Liermann, M. Hanfland, M. Ekholm, Q. Feng, L. V. Pourovskii, M. I. Katsnelson, J. M. Wills, and I. A. Abrikosov, The most incompressible metal osmium at static pressures above 750 gigapascals, Nature (London) **525**, 226 (2015).

[58] C. S. Perreault, N. Velisavljevic, and Y. K. Vohra, High-pressure structural parameters and equation of state of osmium to 207 GPa, Cogent Phys. **4**, 1376899 (2017).

[59] W. J. Evans, M. J. Lipp, H. Cynn, C. S. Yoo, M. Somayazulu, D. Häusermann, G. Shen, and V. Prakapenka, X-ray diffraction and Raman studies of beryllium: Static and elastic properties at high pressures, Phys. Rev. B **72**, 094113 (2005).

[60] R. Torchio, C. Marini, Y. O. Kvashnin, I. Kantor, O. Mathon, G. Garbarino, C. Meneghini, S. Anzellini, F. Occelli, P. Bruno, A. Dewaele, and S. Pascarelli, Structure and magnetism of cobalt at high pressure and low temperature, Phys. Rev. B **94**, 024429 (2016).

[61] O. Tschauner, O. Grubor-Urosevic, P. Dera, and S. R. Mulcahy, Anomalous elastic behavior in hcp- and Sm-type dysprosium, J. Phys. Chem. C **116**, 2090 (2012).

[62] See Supplemental Material at http://link.aps.org/supplemental/10.1103/PhysRevB.100.174107 for animations showing the influence of pressure on the electronic band structure and density of states of Re.

[63] L. F. Mattheiss, Band structure and Fermi surface for rhenium, Phys. Rev. **151**, 450 (1966).

[64] W. Harrison, *Electronic Structure and the Properties of Solids: The Physics of the Chemical Bond*, Dover Books on Physics (Dover, New York, 1989).

[65] B. Fultz, Vibrational thermodynamics of materials, Prog. Mater. Sci. **55**, 247 (2010).

[66] S. Baroni, P. Giannozzi, and E. Isaev, Density-functional perturbation theory for quasi-harmonic calculations, Rev. Mineral. Geochem. **71**, 39 (2010).

[67] A. Otero-De-La-Roza, D. Abbasi-Pérez, and V. Luaña, Gibbs2: A new version of the quasiharmonic model code. II. Models for solid-state thermodynamics, features and implementation, Comput. Phys. Commun. **182**, 2232 (2011).

[68] Z. Wu and R. M. Wentzcovitch, Quasiharmonic thermal elasticity of crystals: An analytical approach, Phys. Rev. B **83**, 184115 (2011).

[69] L. F. Huang, X. Z. Lu, E. Tennessen, and J. M. Rondinelli, An efficient ab-initio quasiharmonic approach for the thermodynamics of solids, Comput. Mater. Sci. **120**, 84 (2016).